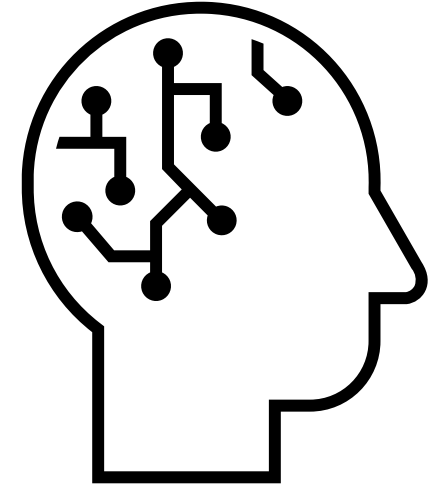




Lung Cancer Screening: is there a role for Artificial Intelligence?



William R. Mayfield MD FACS

Thoracic Surgery

Medical Director Lung Cancer Screening and Incidental Nodule Programs

Medical Director Multi-Disciplinary Oncology Clinics

Wellstar Health System

Disclosures

- Consultant, Philips
- Consultant, Medtronic

Content co-created with
Ilya Gipp, MD PhD

Chief Medical Officer
Imaging and Oncology
at Royal Philips



Overview

- What is Artificial Intelligence?
- Applications of AI in Imaging
- Applications of AI in Lung Cancer
- Future opportunities for AI in Early Detection of Lung Cancer

Artificial intelligence definitions

ML (Machine Learning)

Approach for computers to learn without being explicitly programmed



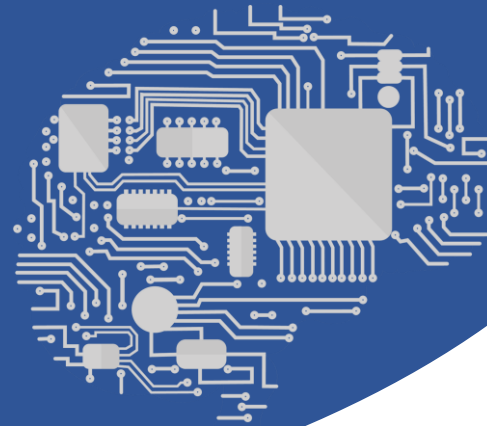
DL (Deep Learning)

Training machines to think like human brains

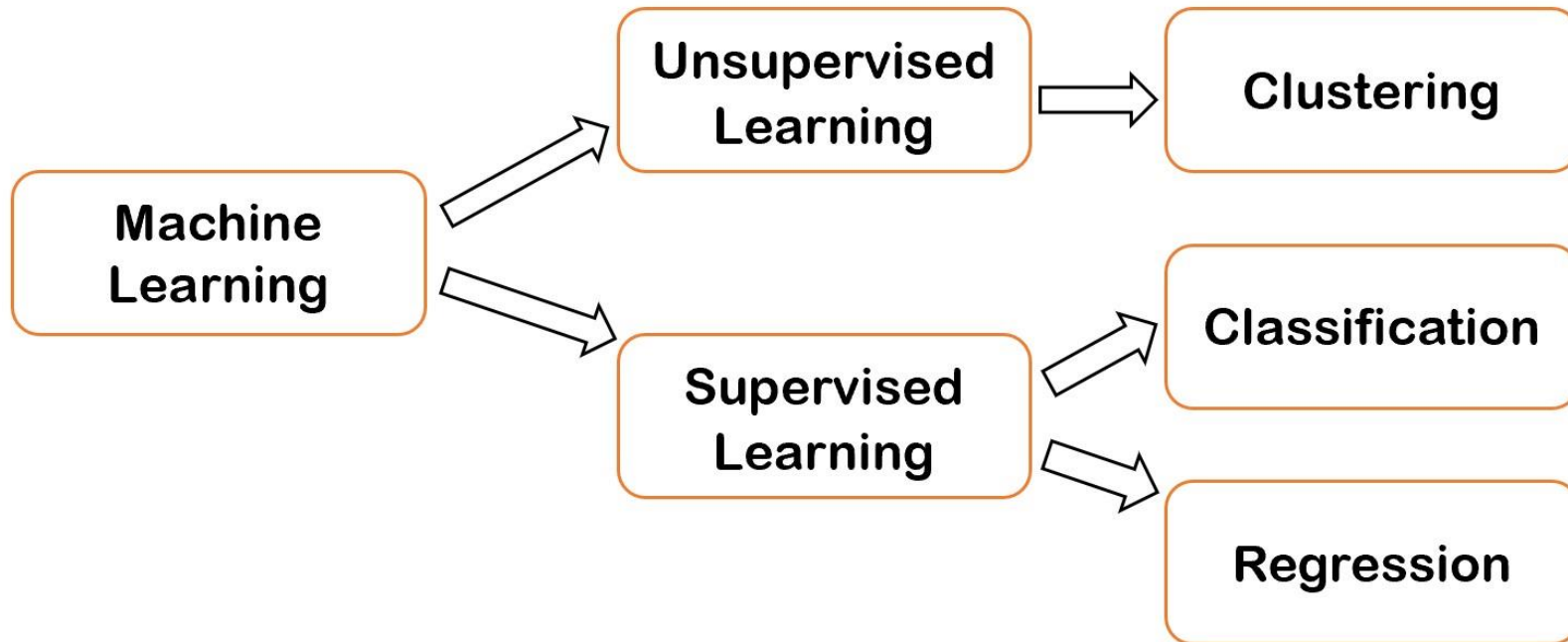


AI (Artificial Intelligence)

Intelligent machines that “think” and act like humans



Machine Learning

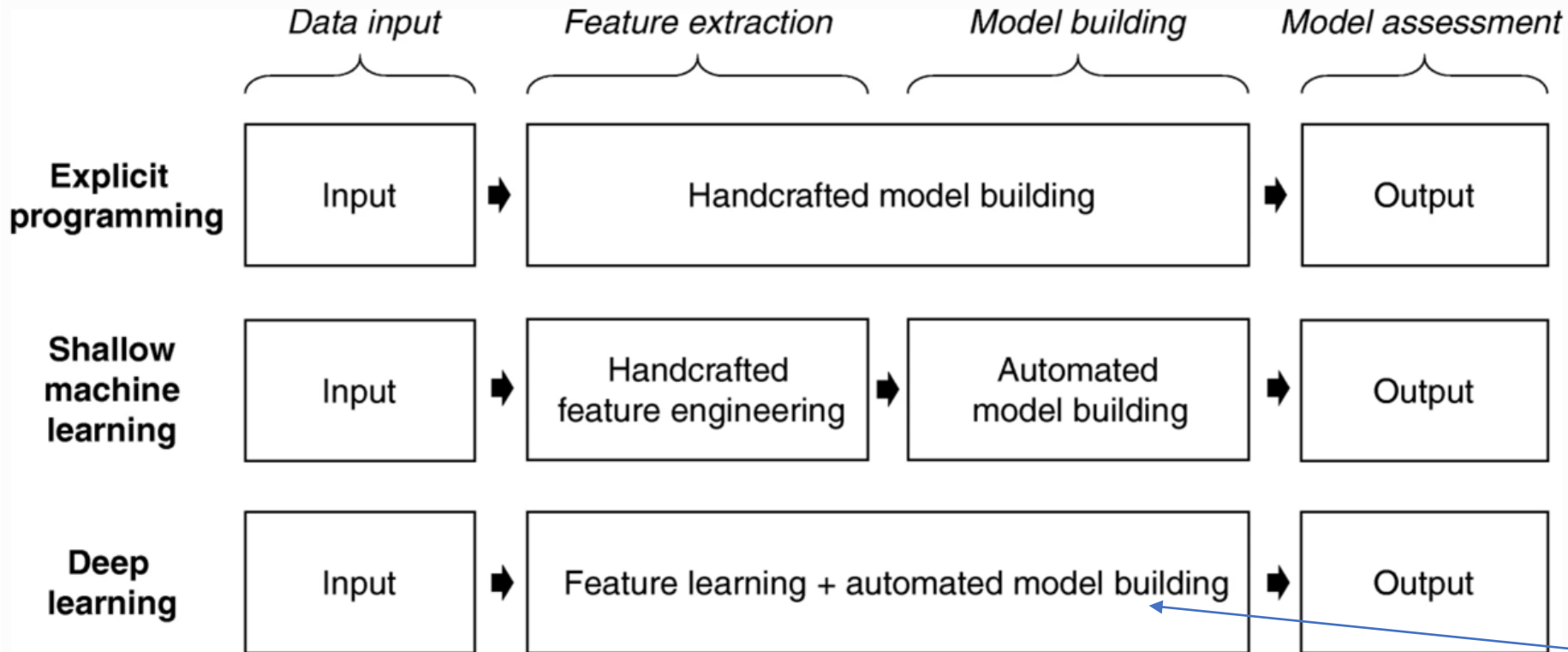


Infer patterns without known outcomes

Data management by written algorithms, known labeled outcomes

Deep Learning

From: [Machine learning and deep learning](#)



Process of analytical model building (inspired by Goodfellow et al. [2016](#), p. 10)

Learns from problem-specific training data to *automate* the process of analytical model building and solve associated tasks.

The machine improves its own performance with time.

Radiology Images are huge amounts of pure digital data

Radiomics: Images Are More than Pictures, They Are Data¹

In the past decade, the field of medical image analysis has grown exponentially, with an increased number of pattern recognition tools and an increase in data set sizes. These advances have facilitated the development of processes for high-throughput extraction of quantitative features that

ORIGINAL RESEARCH ■ SPECIAL REPORT

ORIGINAL RESEARCH ■ SPECIAL REPORT

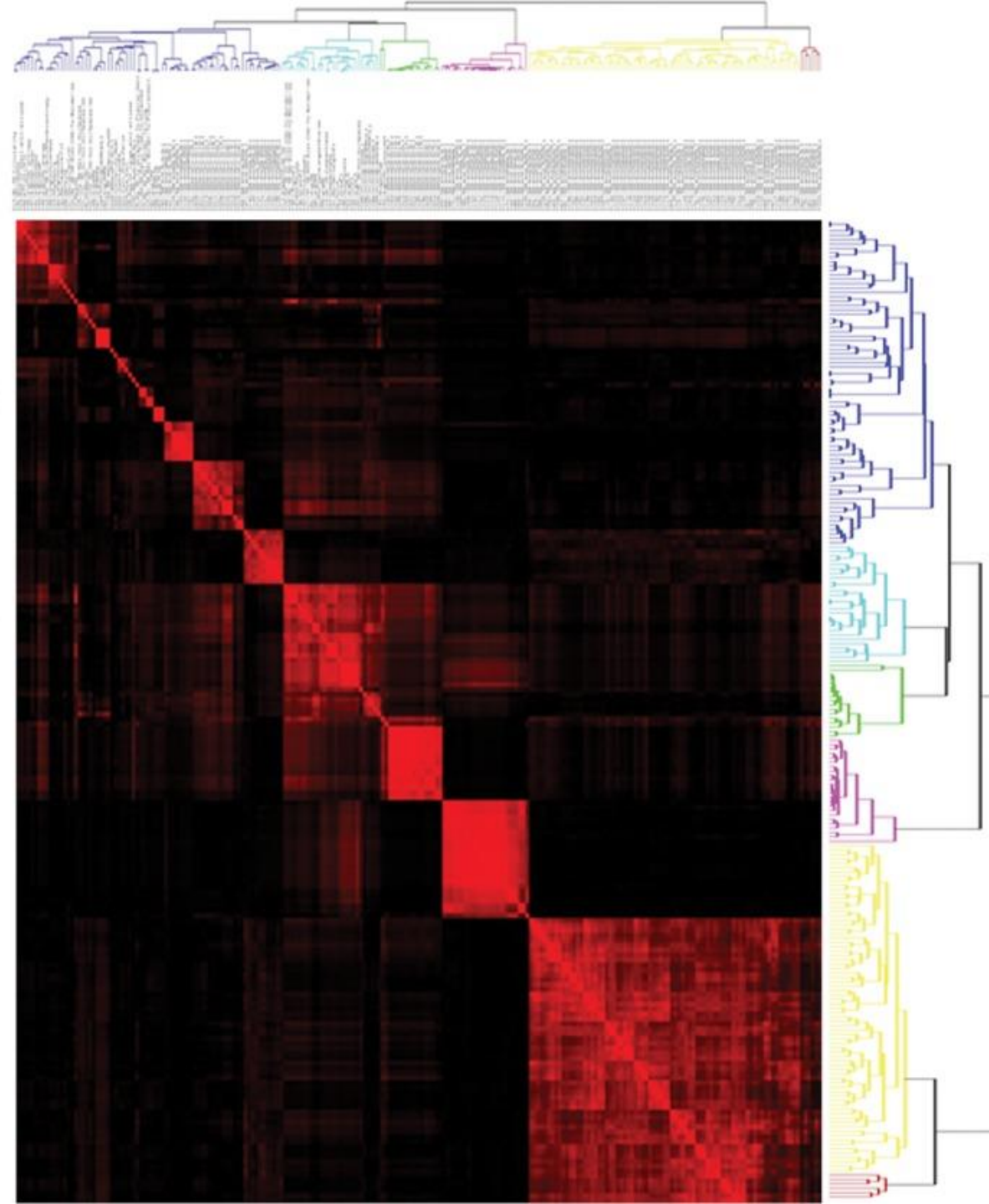
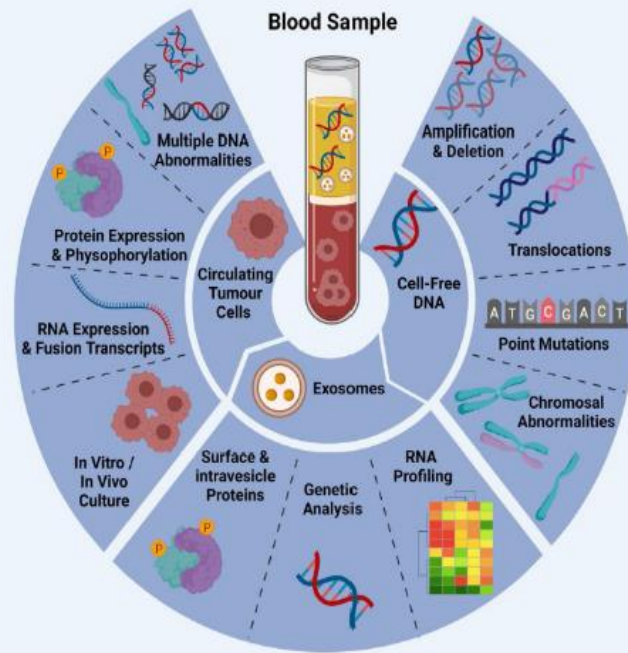
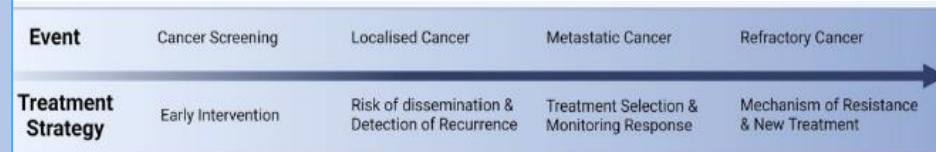


Figure 3: Covariance matrix of radiomic features. A total of 219 features were extracted from each non–small cell lung cancer tumor in 235 patients. Across all tumors, each feature was individually compared with all other features by using regression analysis, thereby generating correlation coefficients (R^2). Individual features were then clustered and plotted along both axes, and R^2 is shown as a heat map, with areas of high correlation ($R^2 > 0.95$) shown

Lung Cancer Care requires huge amounts of data: largely unstructured

Can we gain insights by allowing AI to trend and sort metadata across large populations?

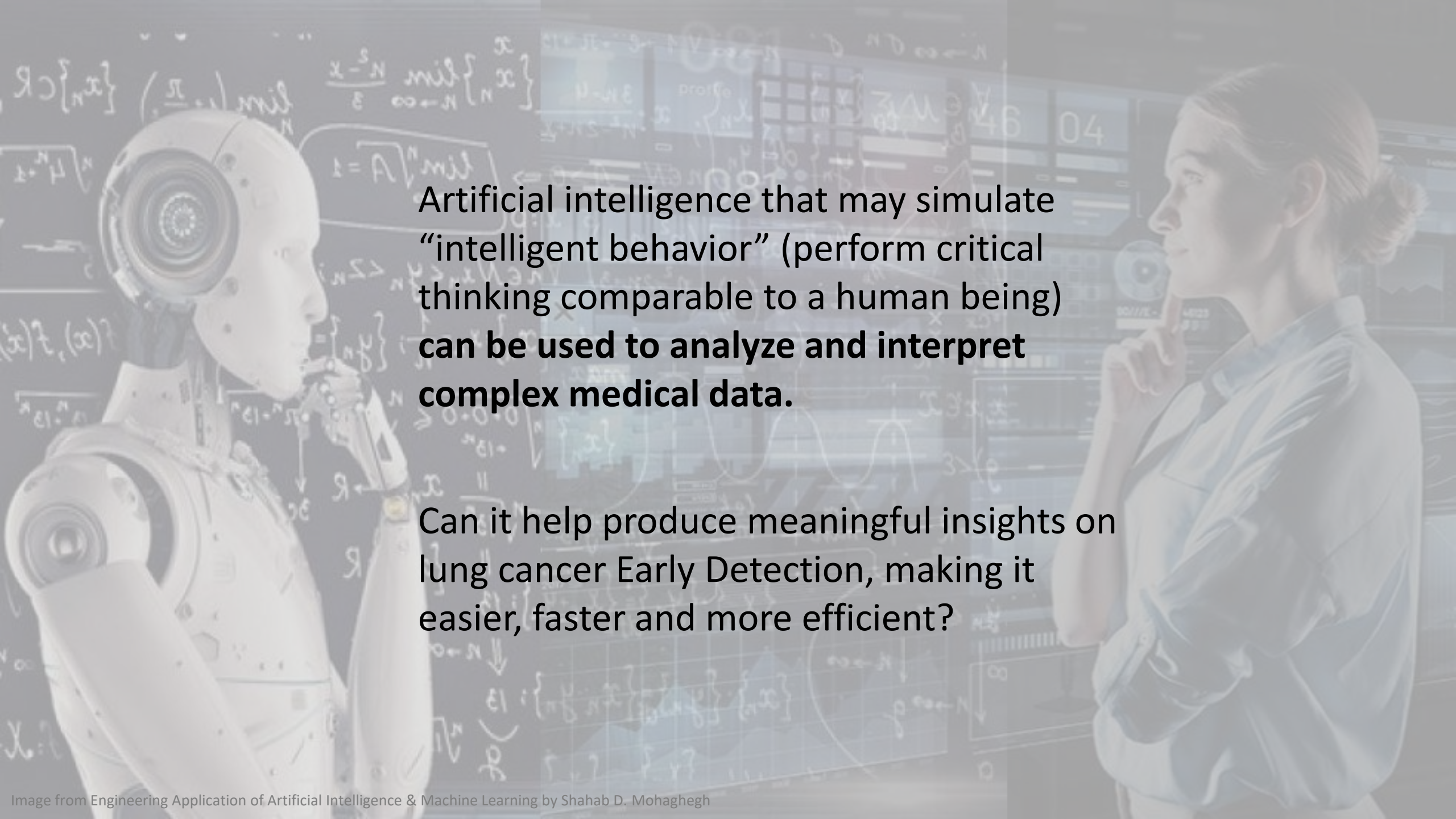
Demographics
 Risk factors
 Health Factors
 Imaging
 Serology tests
 Lung function
 Cardiac Function
 Histology
 Immunohistochemistry
 Biomarkers
 Immune
 Mutations
 Radiation
 Chemotherapies
 Immune Therapies
 Outcomes data
 Follow up data



type	Strength	Weakness	Clinical application in oncology
circulation	<ul style="list-style-type: none"> Reflective of tumor molecular alterations/mutations Stable up to 2 days in blood samples 	<ul style="list-style-type: none"> Contamination of germinal cfDNA Cannot reflect every gene mutation Low amount in plasma Undetectable in many patients with early-stage cancer 	<ul style="list-style-type: none"> Elevated in cancer patients compared to healthy individuals Increases with tumor size and stage
all body	<ul style="list-style-type: none"> Reflective of tumor heterogeneity Highly sensitive assays (NGS, PCR) 	<ul style="list-style-type: none"> Less stable than non-tumor DNA 	
saliva	<ul style="list-style-type: none"> Stable source of tumor genetic material (DNA, RNA, protein, miRNA) Commercial kits available 	<ul style="list-style-type: none"> required standardization for extraction and detection Unreliable isolation procedures 	<ul style="list-style-type: none"> Elevated in cancer patients compared to healthy individuals Exosome size positively correlates with unfavorable outcomes
saliva	<ul style="list-style-type: none"> Assessment of tumor markers (FD-L1) during treatment Demonstration of signal co-localization Cell morphology and functional studies Different profile among early-stage cancer patients Distinguishable between cancer patients and healthy individuals 	<ul style="list-style-type: none"> Not predictive of therapeutic benefit in metastatic setting Undetectable in most patients with early-stage cancer Rare to capture in the bloodstream Loss of epithelial specific markers during epithelial mesenchymal transition (EMT) High variability Lack of standardization Unspecific for a cancer type 	<ul style="list-style-type: none"> Predictive of early relapse after primary treatment CTC number correlates with progression-free survival and overall survival
saliva	<ul style="list-style-type: none"> TEP-RNA is reflective of tumor transcriptome Abundant Dynamic mRNA repertoire because of short life-span 	<ul style="list-style-type: none"> Reproducibility Lack of validated assay 	<ul style="list-style-type: none"> Distinguishable between healthy individuals

The sample type, strength, weakness and clinical applications of each marker is discussed.





Artificial intelligence that may simulate “intelligent behavior” (perform critical thinking comparable to a human being) **can be used to analyze and interpret complex medical data.**

Can it help produce meaningful insights on lung cancer Early Detection, making it easier, faster and more efficient?

First AI applications



WIRED STAFF

SCIENCE JUN 26, 2012 11:15 AM

Google's Artificial Brain Learns to Find Cat Videos

When computer scientists built a neural network of 16,000 connections and let it browse YouTube, it did what many web users might do -- it began to look for cats.

Picking up on the most commonly occurring images featured on YouTube, the system achieved 81.7 percent accuracy in detecting human faces, 76.7 percent accuracy when identifying human body parts and 74.8 percent accuracy when identifying cats.

"The network is sensitive to high-level concepts such as cat faces and human bodies. Starting with these learned features, we trained it to obtain 15.8 percent accuracy in recognizing 20,000 object categories, a leap of 70 percent relative improvement over the previous state-of-the-art [networks]."

Computer-aided lung nodule detection – as a starting point

Radiology

Kyongtae T. Bae, MD, PhD
Jin-Sung Kim, MS²
Yong-Hum Na, MS
Kwang Gi Kim, PhD
Jin-Hwan Kim, MD³

Published online before print
10.1148/radiol.2361041286
Radiology 2005; 236:286–294

Abbreviations:

Pulmonary Nodules: Automated Detection on CT Images with Morphologic Matching Algorithm— Preliminary Results¹

Eur Radiol (2012) 22:2076–2084
DOI 10.1007/s00330-012-2437-y

CHEST

Performance of computer-aided detection of pulmonary nodules in low-dose CT: comparison with double reading by nodule volume



Contents lists available at ScienceDirect

European Journal of Radiology

journal homepage: www.elsevier.com/locate/ejrad

Computer-aided diagnosis (CAD) of subsolid nodules: Evaluation of a commercial CAD system

Joseph Benzakoun (MD)^{a,b,*}, Sébastien Bommart (MD PhD)^{c,d}, Joël Coste (MD PhD)^{a,b},
Guillaume Chassagnon (MD PhD)^{b,e}, Mathieu Lederlin (MD PhD)^{f,g},
Samia Boussouar (MD)^{b,h}, Marie-Pierre Revel (MD PhD)^{b,e}

With early CADe tools, Bae et al. in **2005** reported a **sensitivity of 95.6%** for the detection of pulmonary nodules nonetheless **with a number of false positives per examination of 6.9 and 4.0** for detection sensitivity thresholds of 3 and 5 mm, respectively

Source: Radiology 2005; 236:286–294

*"Commercially available CADe tool has **sensitivity of 96.7%**, whereas **double reading has only 78.1% sensitivity**. Nonetheless, these CADe tools are known to encounter a **high number of false positives** and insufficient performances for the detection of subsolid nodules"*

Source: Eur Radiol (**2012**) 22:2076–2084

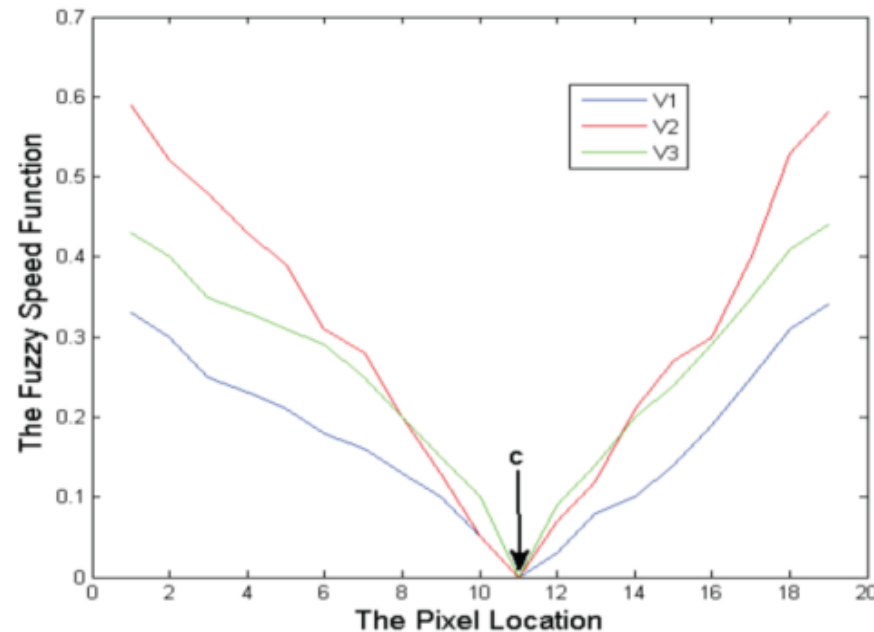
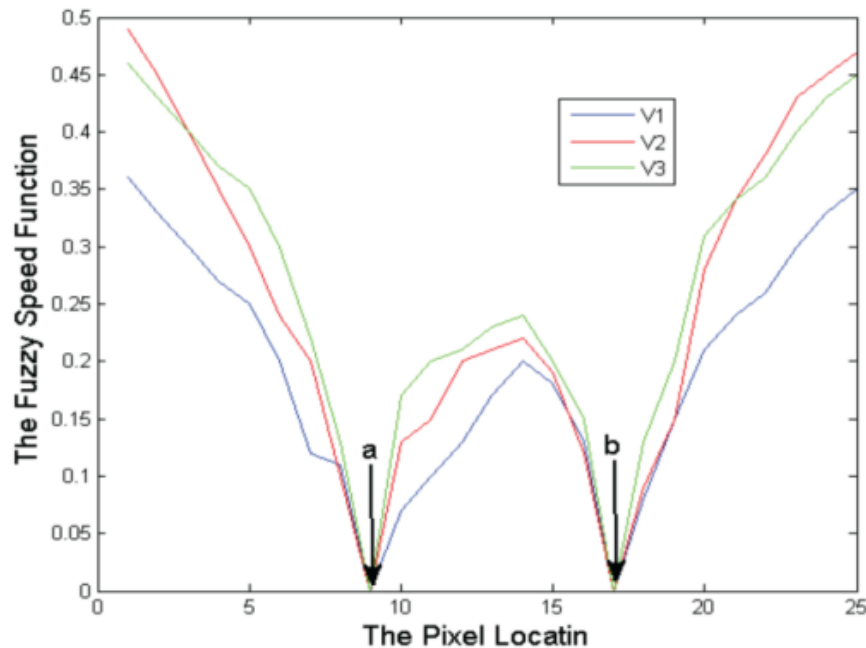
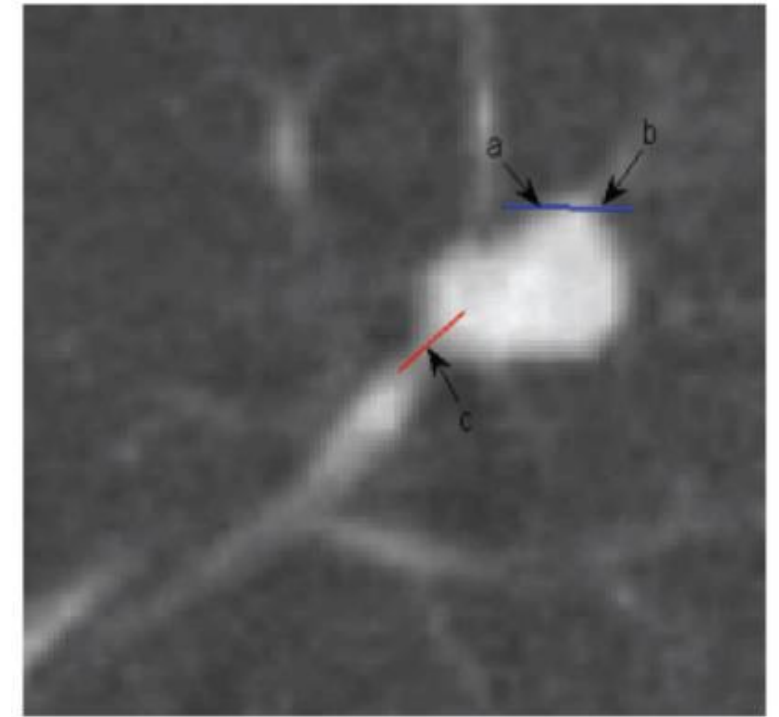
*"With sensitivity adjusted for 3-mm nodule detection, **50%** of subsolid nodules were detected, **26%** at the 5-mm setting. And at the highest sensitivity setting (2-mm nodule detection), the nodule detection rate only increased to **54%**"*

Source: European Journal of Radiology 85 (**2016**) 1728–1734



Fuzzy Speed Function Based Active Contour Model for Segmentation of Pulmonary Nodules

Kan Chen, Bin Li^{*}, Lian-fang Tian, Wen-bo Zhu and Ying-han Bao
School of Automation Science and Engineering, South China University of Technology, Guangzhou, Guangdong, China





Data Science Bowl 2017

Can you improve lung cancer detection?

\$1,000,000

Prize Money



Booz Allen Hamilton · 1,972 teams · 6 years ago

A total of US\$1 million in prize money for the ten best algorithms that could predict lung cancer from a single screening CT scan. The task was to predict whether an individual patient would be diagnosed with lung cancer within 1 year of the scan

2017 Data Science Bowl winners include:


- First Place: Liao Fangzhou and Zhe Li, two researchers from China's Tsinghua University who have no formal medical background but were able to apply their analytics skills to an unfamiliar but challenging area of research.
- Second Place: Julian de Wit and Daniel Hammack, both software and machine learning engineers based in the Netherlands. Julian came in **third in the Data Science Bowl 2016**.
- Third Place: Team Aidence, members of which work for a Netherlands-based company that applies deep learning to medical image interpretation.

Google AI project 2019



analysis, into a product currently remains to be seen. All of the solutions developed by Google AI so far are proprietary. In the *Nature Medicine* letter, the authors state that their code has “dependencies on internal tooling, infrastructure and hardware, and its release is therefore not feasible. However, all experiments and implementation details are

Google's lung cancer AI: promising tool that needs further validation

by Armin Arora and Bram van Ginneken 

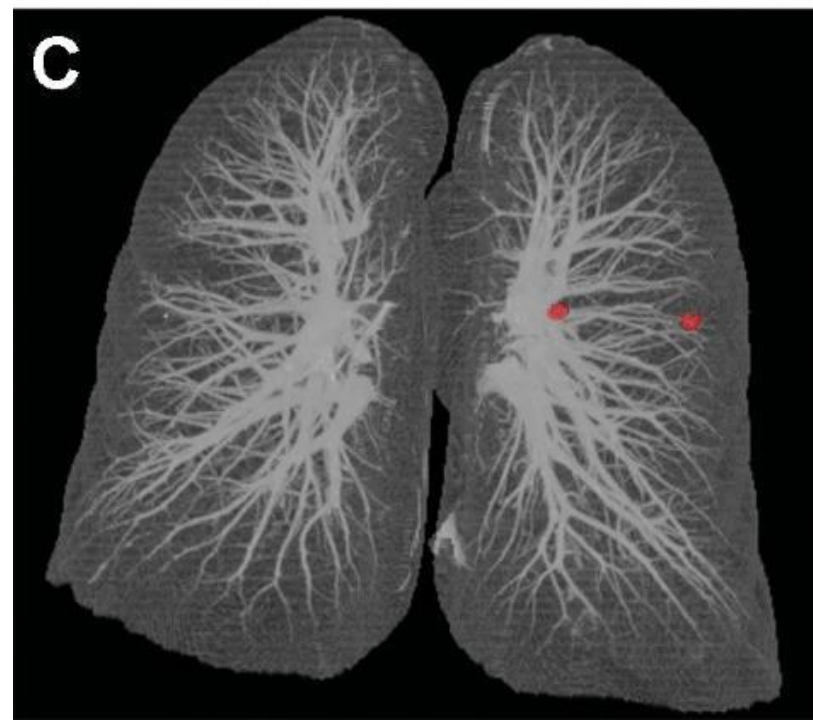
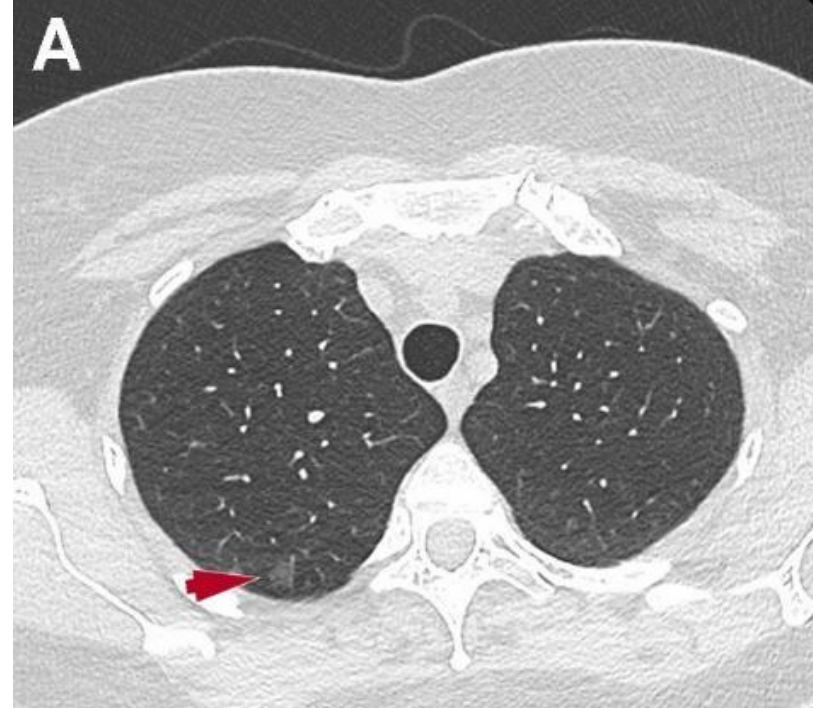
Researchers from Google AI have presented results obtained using a **deep learning model** for the detection of lung cancer in screening CT images. **The authors report a level of performance similar to, or better than, that of radiologists.** However, these claims are currently too strong. The model is promising but needs further validation and could only be implemented if screening guidelines were adjusted to accept recommendations from black-box proprietary AI systems.

Refers to Ardila, D. et al. End-to-end lung cancer screening with three-dimensional deep learning on low-dose chest computed tomography. Nat. Med. 25, 954–961 (2019).

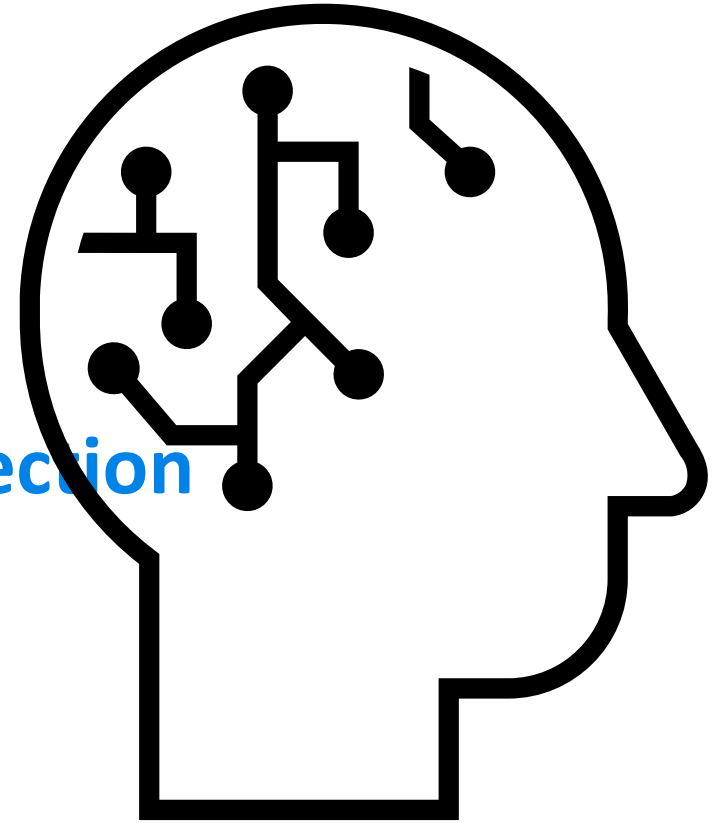
Deep Learning vs. Machine Learning 2022

Detection of a pulmonary ground-glass nodule. **A** Axial chest CT image shows a 10 × 8 mm ground-glass nodule (arrow) in the right upper lobe. **The ground-glass nodule is not detected by two different computer-aided detection tools based on classical machine learning methods (B and C) but is correctly detected by the one based on deep learning (D)**

Source: Artificial intelligence in lung cancer: current applications and perspectives - Japanese Journal of Radiology (November 9, 2022)



Current applications of AI in Early Detection



2015 COMPUTER-AIDED NODULE DETECTION

DynaCAD Lung

Advanced visualization for CT chest exams



DynaCAD Lung is a vendor neutral Computer-Aided Detection (CAD) system that provides a robust set of automated tools for radiologists to analyze multi-slice CT exams of the chest.

- Standard CT scans
- Comparison to prior exams
- Standardized nodule table (structured data)

NATURAL LANGUAGE PROCESSING TO DETECT INCIDENTAL FINDINGS



Wellstar Incidental Nodule
2019-2022 (800 days)

92,000 Chest Imaging Reports referred by
NLP to reviewers

Released By: KEVIN S EARLY, MD 9/17/2020 12:50 AM The Results Reporting Office (F1) will complete appropriate follow-up actions based on defined processes. F1 EXAM: KH CT ABDOMEN/PELVIS W/O IV CONTRAST TECHNIQUE: CT scan of the abdomen and pelvis with multiplanar reformatted images generated from the data set without IV contrast. Dose reduction techniques were utilized. CLINICAL INDICATION: urinary frequency, incontinence and hematuria. Pain FINDINGS: COMPARISON: No comparison studies are available at this time. Liver: Hepatic steatosis. Lower chest: 5 mm pleural-based noncalcified pulmonary nodule left lower lobe image 15. Additional smaller pulmonary nodules are seen in the left lower lobe. Pancreas: Normal. Gallbladder: Normal. Adrenals: Normal. Spleen: Normal. Gastrointestinal: The stomach, small bowel, and colon appear normal. The appendix is not identified, but there is no evidence of inflammation. Kidneys: 3 mm calculus in the right kidney, nonobstructing.. No evidence of hydronephrosis. Left kidney normal. Vasculature: Abdominal and pelvic vasculature appears normal on unenhanced images. Pelvis: Prostate and seminal vesicles are normal. Bones: No destructive osseous lesion. Lymph nodes: No enlarged lymph nodes. Nonobstructing right renal calculus IMPRESSION: . . of the chest at 12 months could be performed. There are noncalcified solid and/or part solid nodules as above. Per 2017 Fleischner Society guidelines, the recommendation for a patient with multiple < 6 mm noncalcified nodules is usually no followup scan. In a high risk patient, optional (



2021 AI assisted DIAGNOSIS



ABOUT US ▾

PRODUCTS & SOLUTIONS ▾

RESOURCES ▾

NEWS & EVENTS

US PRESS RELEASE: Optellum Receives FDA Clearance for the World's First AI-Powered Clinical Decision Support Software for Early Lung Cancer Diagnosis

Rhiannon Lassiter - March 23, 2021 - Clinical / News and PR

- AI-powered Radiomics-based *digital biomarker* for lung cancer
- Features a clinically-validated Lung Cancer Prediction (LCP) score
- The score is computed from full patterns of 3D pixels in standard CT images
- Deployed inside “Lung Cancer Orchestrator” Nodule Clinic App

Future for Screening: Machine Learning of VOCs



Article

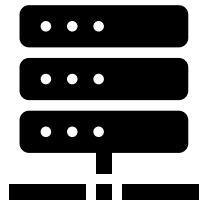
A Study of Diagnostic Accuracy Using a Chemical Sensor Array and a Machine Learning Technique to Detect Lung Cancer

Chi-Hsiang Huang^{1,2}, Chian Zeng³, Yi-Chia Wang^{1,2}, Hsin-Yi Peng³, Chia-Sheng Liu^{3,5}  and Hsiao-Yu Yang^{3,6,*} 

Characteristics	Lung Cancer Cases (n = 56)	Non-Tumour Controls (n = 188)
Age (year), mean (SD)	65.3 (8.8)	53.5 (16.1)
Male, no. (%)	12 (21.4)	106 (56.4)
Cigarette smoking		
Pack-years, mean (SD)	21.0 (10.7)	20.6(18.3)
Smoking status		
Current smokers, no. (%)	2 (3.6)	25 (13.3)
Former smokers, no. (%)	8 (14.3)	11 (5.9)
Never smoked, no. (%) ^a	44 (78.6)	150 (79.8)
Second-hand smokers (%)	2 (3.6)	2 (1.1)
Tumour histological type		
Squamous cell carcinoma, no. (%)		1 (1.8%)
Adenocarcinoma, no. (%)		52 (92.9%)
Small cell lung cancer, no. (%)		1 (1.8%)
Other carcinomas, no. (%)		2 (3.6%)
Clinical stage		
I		37 (66.1%)
II		7 (12.5%)
III		11 (19.6%)
IV		1 (1.8%)

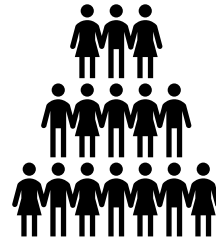


Opportunities for AI in Lung Cancer



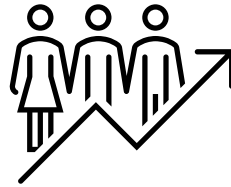
Data management

- Convert unstructured data to Structured
- Collate relevant data for work-up and treatment



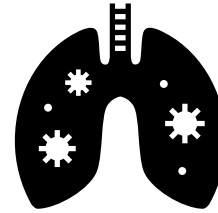
Population Health

- Refine Population Risk assessment
- Refine Lung Screening criteria
- Address Social Determinants of Health



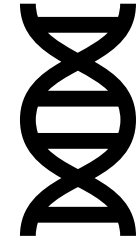
Risk stratification

- Refine Lung Screening criteria
- Refine NLP referral for review
- Address Social Determinants of Health



Nodule Management

- Improved specificity in nodule detection
- Improved sensitivity for GGOs



Treatment and Outcomes

- Determine best treatment based on all factors known
- Predict outcomes based on all factors known

For example

Volumes of Patient Data are very high to detect 1 lung cancer



Lung Screening

33,645 scans

11,866 unique patients

406 Lung Cancers

55 non-lung cancers

Incidental Nodule

2019-2022 (800 days)

92,000 Imaging Reports referred by NLP to reviewers

35,000 Imaging Reports referred to NP and RN for review

1014 cases reviewed by Physicians

76 Lung Cancers detected and treated

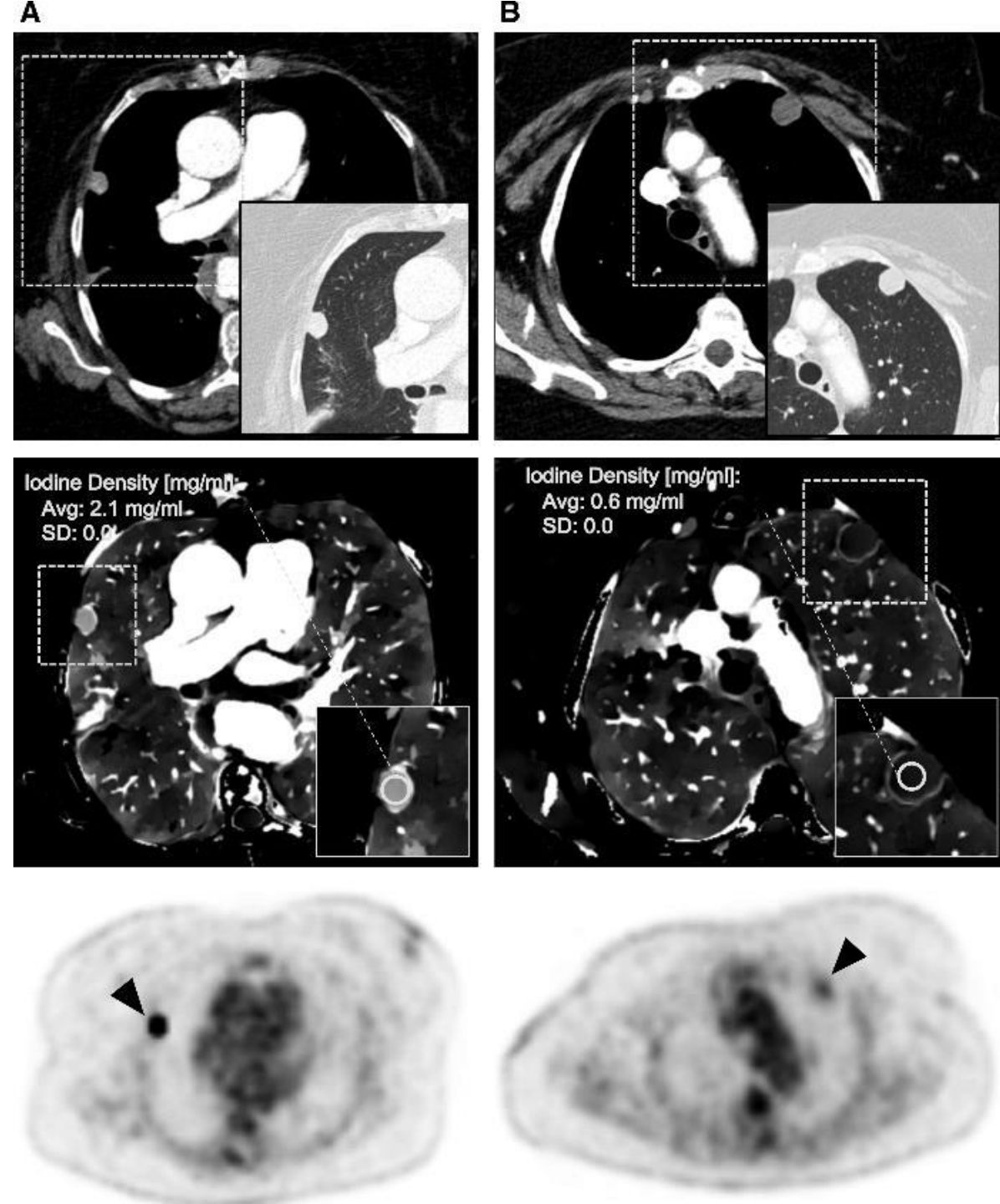
14 non-lung cancers

New tool: Spectral CT

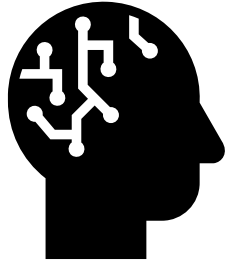
Conventional CT images (upper row) show two pulmonary nodules in the right (A) and left (B) upper lobe, both of which are considered **suspicious for malignancy based on their size and appearance**.

Iodine maps available from **dual-layer, dual-energy CT** (center row) clearly indicate significant **uptake of the iodinated contrast media** by the right pulmonary nodule (**A, 2.1 mg/ml**), whereas the left pulmonary nodule did not take up iodine (**B, 0.6 mg/ml**).

Concordant findings were obtained on FDG18 – PET (lower row), with low hypermetabolic activity associated with the left pulmonary nodule (maximum standardized uptake value = 1.7, arrowhead in B), and the right nodule demonstrating significant fludeoxyglucose avidity (maximum standardized uptake value = 7.1, arrowhead in A).

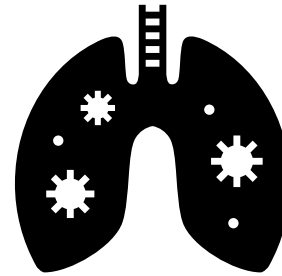


Summary



Artificial Intelligence has several forms:

Machine Learning
Deep Learning
Artificial Intelligence



There are several applications already in clinical practice

NLP
Computer-aided Detection
Radiomics Digital biomarker



Unsolved problems remain

Unstructured data
Population Health
Risk assessment improvement